

Supplementary Information for

Antifreeze Protein Mimetic Metallohelices with Potent Ice Recrystallization Inhibition Activity

**Daniel E. Mitchell¹, Guy J Clarkson,¹ David J. Fox,¹ Rebecca A. Vipond, Peter Scott^{1*}
and Matthew I. Gibson^{1,2*}**

¹Department of Chemistry, University of Warwick, Coventry, UK, CV4 7AL.

²Warwick Medical School, University of Warwick, Coventry, UK, CV4 7AL.

Contents

General Synthetic Details	S2
Physical & Analytical Details	S2
Syntheses	S3
Ice recrystallisation inhibition (splat) assay.	S6
Molecular structure of Zn(II) perchlorate analogue of 6	S7
Location of counter-ions and solvent in crystal structures	S9
Hydrophobicity calculations	S13

Synthetic details

All solvents and chemicals purchased from commercial sources (Sigma-Aldrich, Acros, Fisher Scientific or Alfa Aesar) were used without further purification unless otherwise stated. Deuterated solvents were purchased from Sigma-Aldrich and Cambridge Isotope Laboratories.

Enantiomers of compounds **1-3** and **6**¹ and 1-phenyl-2-(prop-2-ynoxy)ethanamine,² and 5-(2,2'-bipyridin-5-ylmethoxy)picolinaldehyde¹ were prepared by reported methods.

Physical and Analytical Details

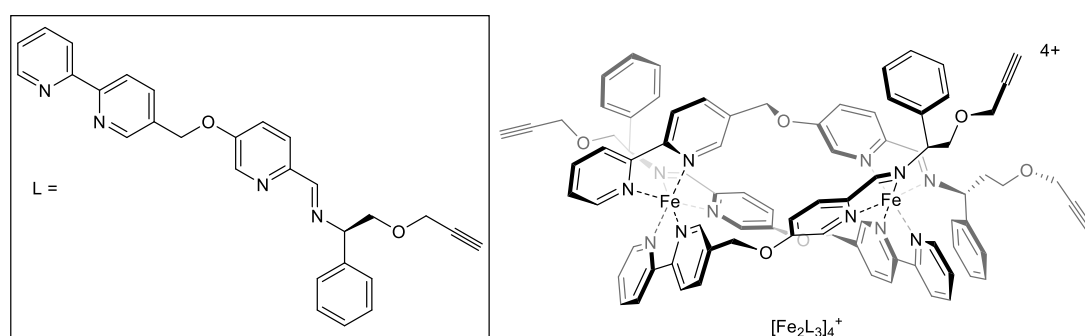
NMR spectra were recorded on Bruker Spectrospin 300/400/500 MHz spectrometers. Routine NMR assignments were confirmed by ¹H-¹H (COSY) and ¹³C-¹H (HMQC) correlation experiments where necessary. The spectra were internally referenced using the residual protic solvent (CDCl₃, CD₃CN etc.) resonance relative to tetramethylsilane ($\delta = 0$ ppm). ESI mass spectra were recorded on an Agilent Technologies 1260 Infinity spectrometer or a Bruker Daltonics MicroTOF spectrometer. Infra-Red spectra were measured using a Bruker Alpha-P FTIR spectrometer. Elemental analyses were performed by Medac Ltd. Chobham, Surrey GU24, 8JB, UK or Warwick Analytical Service, Coventry, CV4 7EZ. Optical rotation measurements were performed on a Perkin Elmer Polarimeter 341 by Warwick Analytical Services, Coventry, UK. In all cases the following parameters were used: solvent methanol, temperature 20 °C, pathlength 100 mm, wavelength 589 nm. Thermogravimetric analysis (DSC1-1600 scanning calorimeter) was used to determine the amount of water of crystallisation present in the chloride salts of iron (II) triplex metallolohelices.

The presence of water of crystallisation in metallolohelix compounds was confirmed by NMR and IR spectroscopy and the absence of other solvents was confirmed also by NMR. The

hydration number was then determined by thermogravimetric analysis (Mettler-Toledo DSC1-1600 scanning calorimeter) and the relevant mass loss was correlated with microanalytical data.

Syntheses

$\Delta_{\text{Fe}}\text{-}[\text{Fe}_2\text{L}_3]\text{Cl}_4\cdot 9\text{H}_2\text{O}$ ($\Delta\text{-4}$)



5-(2,2'-bipyridin-5-ylmethoxy)picolinaldehyde (0.20 g, 0.69 mmol) and (S)-1-phenyl-2-(prop-2-ynyloxy)ethanamine (0.08 g, 0.69 mmol) were dissolved in methanol. Iron (II) chloride (0.06 g, 0.46 mmol) was added and an immediate colour change to deep magenta was seen. The solution was heated at reflux (75°C) for 48 h. The solution was filtered through a small pad of Celite and the solvent was removed under reduced pressure to yield a dark purple solid.

Yield 0.243 g, 80 %.

Elemental analysis found (calculated for $\text{C}_{84}\text{H}_{72}\text{Cl}_4\text{Fe}_2\text{N}_{12}\text{O}_6\cdot 9\text{H}_2\text{O}$) % C 57.69 (57.29), H 4.89 (5.15), N 9.39 (9.54). Mass loss at 450 °C 9% (calc 9.2%)

$^{13}\text{C}\{^1\text{H}\}$ NMR (126 MHz, 298 K, MeOH) δ_{C} 172.0, 171.8, 171.3 (CHN), 161.1, 160.9, 160.8, 160.5, 160.3, 160.0, 159.4, 158.8, 158.2, 157.7, 157.1, 155.0, 153.8, 153.7, 153.5, 140.4, 139.8, 136.8, 136.6, 135.8, 135.1, 134.9, 133.8, 133.0, 132.6, 130.5, 130.3, 130.0, 130.0, 129.7, 129.6, 129.5, 129.1, 128.8,

128.4, 127.5, 127.4, 127.3, 127.1, 125.8, 125.3, 125.1, 125.0, 124.8, 124.7 (Ar), 77.6, 77.2, 77.0 (CH₂), 73.5, 73.3, 72.7 (CH), 71.9, 71.7, 71.3 (CH₂), 70.7, 69.6, 69.4 (CCH), 59.7, 59.5, 59.4 (CCH).

MS (ESI) m/z 364 [Fe₂L₃]⁴⁺, 449 [L+H]⁺.

IR ν cm⁻¹ 3362 br s, 3024 m, 1556 m, 1434 w, 1233 m, 1082 m, 700 m.

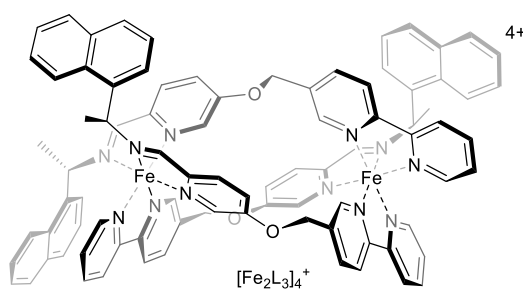
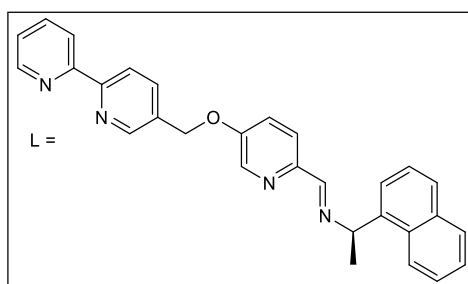
Synthesis $\Delta_{\text{Fe}}\text{-}[\text{Fe}_2\text{L}_3]\text{Cl}_4\cdot 9\text{H}_2\text{O}$ ($\Delta\text{-4}$)

This was prepared in the same manner as the Φ enantiomer, using (*R*)-1-phenyl-2-(prop-2-ynyloxy)ethanamine and gave identical spectra. Thermogravimetric and microanalytical data are consistent with the presence of a nonahydrate.

Yield 0.222 g, 74 %.

Elemental analysis found (calculated for C₈₄H₇₂Cl₄Fe₂N₁₂O₆·9H₂O) % C 56.68 (57.29), H 4.85 (5.15), N 9.29 (9.54).

Synthesis $\Lambda_{\text{Fe}}\text{-}[\text{Fe}_2\text{L}_3]\text{Cl}_4\cdot 8\text{H}_2\text{O}$ ($\Lambda\text{-6}$)



This was prepared in the same manner as the $\Lambda\text{-4}$ using (*R*)-1-(naphthalen-1-yl)ethan-1-amine.

Thermogravimetric and microanalytical data are consistent with the presence of an octahydrate.

Yield 0.267 g, 89 %.

Elemental analysis found (calculated for $C_{87}H_{72}Cl_4Fe_2N_{12}O_3 \cdot 8H_2O$) % C 60.47 (60.36), H 5.05 (5.12), N 9.14 (9.71). Mass loss at 450 °C 8% (calc 8.3%)

$^{13}C\{^1H\}$ NMR (126 MHz, 298 K, MeOH) δ_C 172.7, 172.2, 171.7 (CHN), 161.1, 161.9, 160.5, 160.4, 160.0, 159.7, 158.9, 157.7, 156.5, 155.4, 153.6, 153.4, 151.8, 149.5, 148.6, 148.5, 148.4, 148.3, 147.9, 147.4, 144.7, 142.8, 142.3, 141.2, 141.0, 140.6, 140.2, 140.0, 137.2, 137.1, 136.9, 136.6, 134.0, 133.4, 132.9, 130.6, 129.9, 129.6, 129.0, 128.9, 127.6, 127.5, 126.9, 125.2, 125.1, 125.1, 124.9, 124.8, 124.7, 124.4, 123.3, 122.8, 122.4 (Ar), 70.5 (CH₂), 69.8 (CH), 69.6, 69.5 (CH₂), 68.8, 68.7 (CH), 27.1, 25.9, 25.0 (CH₃).

MS (ESI) m/z 467 [L+Na]⁺, 493 [Fe₂L₃][Cl]³⁺

IR ν cm⁻¹ 3364 br s, 2973 m, 1568 w, 1510 w, 1228 m, 1074 m, 702 w, 621 w.

Synthesis Δ_{Fe} -[Fe₂L₃]Cl₄·8H₂O (Δ -6)

This was prepared in the same manner as the Λ enantiomer, using (*S*)-1-(naphthalen-1-yl)ethan-1-amine and gave identical spectra. Thermogravimetric and microanalytical data are consistent with the presence of an octahydrate.

$\Delta_{Fe,HHT}$ -[Fe₂L⁵₃]Cl₄ was synthesised using the procedure described for $\Lambda_{Fe,HHT}$ -[Fe₂L⁵₃]Cl₄, substituting (*R*)-1-phenylethan-1-amine for (*S*)-1-phenylethan-1-amine.

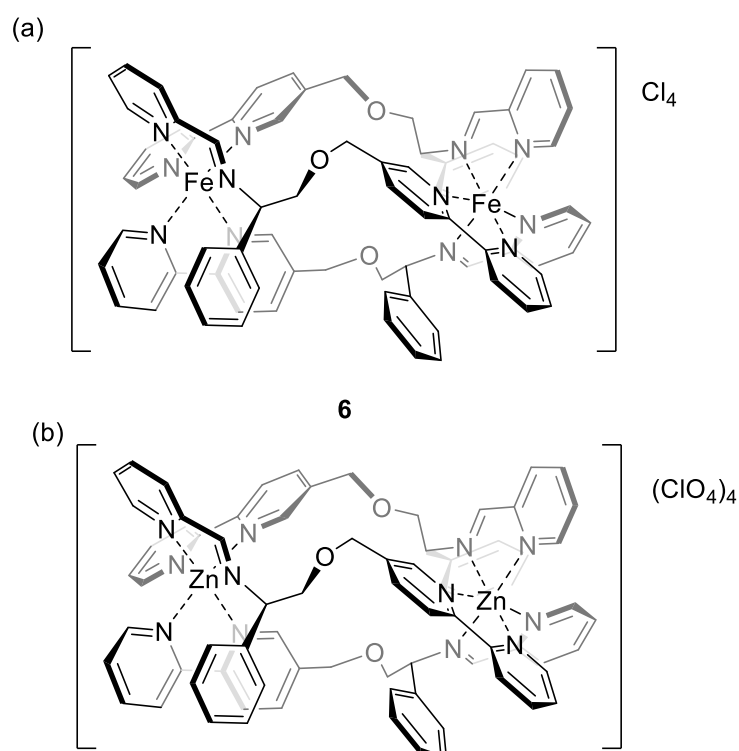
Yield 0.211 g, 77 %.

Ice Recrystallisation Inhibition Assay

Ice recrystallisation inhibition was measured using a modified splay assay.³ A 10 μL sample of polymer dissolved in PBS buffer (pH 7.4) was dropped 1.40 m onto a chilled glass coverslip sat on a piece of polished aluminium placed on dry ice. Upon hitting the chilled glass coverslip, a wafer with diameter of approximately 10 mm and thickness 10 μm was formed instantaneously. The glass coverslip was transferred onto the Linkam cryostage and held at $-6\text{ }^{\circ}\text{C}$ under N_2 for 30 minutes. Photographs were obtained using an Olympus CX 41 microscope with a UIS-2 20 \times /0.45/ ∞ /0-2/FN22 lens and crossed polarizers (Olympus Ltd, Southend on sea, UK), equipped with a Canon DSLR 500D digital camera. Images were taken of the initial wafer (to ensure that a polycrystalline sample had been obtained) and after 30 minutes. Image processing was conducted using Image J, which is freely available.⁴ In brief, ten of the largest ice crystals in the field of view were measured and the single largest length in any axis recorded. This was repeated for at least three wafers and the average (mean) value was calculated to find the largest grain dimension along any axis. The average of this value from three individual wafers was calculated to give the mean largest grain size (MLGS). This average value was then compared to that of a PBS buffer negative control.

Molecular structure of Zn(II) perchlorate analogue of **6**

The water-soluble compounds such as **6** [see (a) below] resist formation of sufficiently large single crystals for X-ray diffraction so we turned to the isostructural Zn(II) perchlorate analogue (b) (see ref 1 for synthesis and characterisation of this compound). Single crystals were grown from acetonitrile/ethyl acetate. A suitable crystal was selected at the UK National Crystallographic Service⁵ and mounted using a MiTeGen loop using Fomblin on a 3-circle AFC11 with a Rigaku Saturn944+ (2x2 bin mode) CCD.



The crystal was kept at 100.15 K during data collection. Using Olex2,⁶ the structure was solved with the ShelXS⁷ structure solution program using Direct Methods and refined with the ShelXL⁸ refinement package using Least Squares minimisation.

Crystal Data for C₈₄H_{81.5}Cl₄N_{14.5}O₂₂Zn₂ ($M = 1918.67$ g/mol): monoclinic, space group C2 (no. 5), $a = 36.032(8)$ Å, $b = 13.162(3)$ Å, $c = 18.767(4)$ Å, $\beta = 99.699(7)^\circ$, $V = 8773(3)$ Å³, $Z = 4$, $T = 100.15$ K, $\mu(\text{CuK}\alpha) = 2.478$ mm⁻¹, $D_{\text{calc}} = 1.453$ g/cm³, 45035 reflections measured ($4.776^\circ \leq 2\theta \leq 133.182^\circ$), 15293 unique ($R_{\text{int}} = 0.0651$, $R_{\text{sigma}} = 0.0476$) which were used in all calculations. The final R_1 was 0.0733 ($I > 2\sigma(I)$) and wR_2 was 0.2069 (all data).

The asymmetric unit contains the complex, one molecule of ethyl acetate, two fully occupied and one half occupied acetonitrile molecules, three fully occupied perchlorate anions and two half-occupied perchlorates. The acetonitrile N300-C302 was refined isotropically at half occupancy. Perchlorate Cl30 was modeled as disordered over two positions related by rotation around the Cl30-O31 bond. The occupancies were fixed at 50:50 and the disordered components refined isotropically. Perchlorate Cl40 sits just off the cell wall and was refined under a Part -1 instruction at 50% occupancy. Perchlorate Cl50 sits on a 2 fold axis and was refined at half occupancy. Four positions were located for the oxygen atoms (O51-O54 refined isotropically at 50% occupancy) which under the action of the two fold axis form a perchlorate disordered over two positions around Cl50. Some additional electron density was modeled as a water molecule disordered over three very closely related positions (too close to be bonded), each position was refined isotropically at a third occupancy. No hydrogens were located for the disordered water.

Many SIMU, DELU and DFIX restraints were used to give the disordered components chemically sensible bond lengths, angles and thermal parameters.

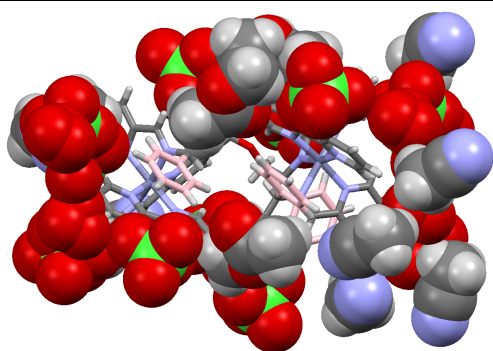
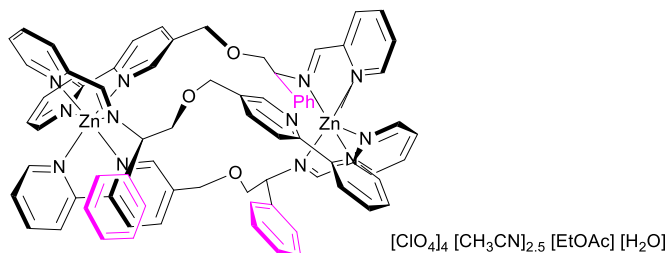
The refinement gave values of Hooft y : 0.080(5) (Olex2) and Flack x : 0.038(8) (Shelxl 2016). Since the Flack parameter deviates from zero by slightly greater than 3σ , the refinement was completed with TWIN/BASF instruction as an inversion twin. The synthesis was undertaken with starting material of a known handedness and the error on the Flack parameter is not unexpected for data from weakly diffracting crystals.

Location of counter-ions and solvent in crystal structures

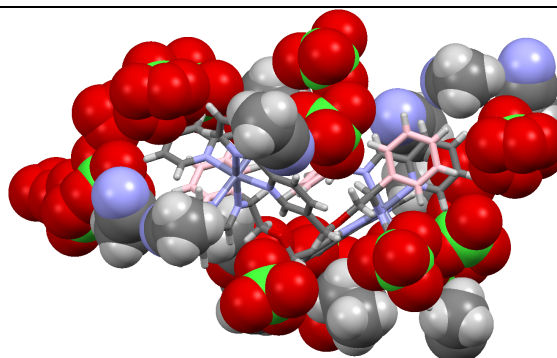
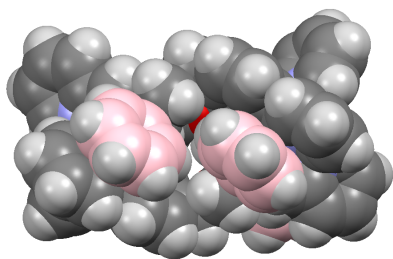
CIF files for a range of structures including the Zn(II) perchlorate analogue of **6** were analysed using Cambridge Crystallographic Data Centre software Mercury (v3.8). For each structure, short contacts were calculated (distances $<$ sum of VdV radii) and any non-hydrocarbon contacts (i.e. solvents, counter-anions) were selected and visualised. Plots below for selected examples are made with the cation skeleton in stick mode and with counter-ions and solvents shown in spacefill mode. Views are oriented to show the region surrounding each pendant π - π arene stack (colourised pink) and also with sample views of other orientations.

Bimetallic "triplex" Zn complex

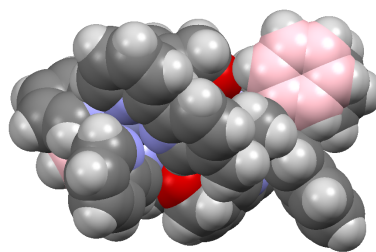
(This work – Zn(II) perchlorate analogue of compound 6)



From most perspectives, the cationic structure is uniformly surrounded by perchlorate anions and solvents. In this view for example, looking down on two π -stack edges, the pendant arene faces have short contacts with ethyl acetate molecules. The same view of the cation in spacefill mode is shown below.



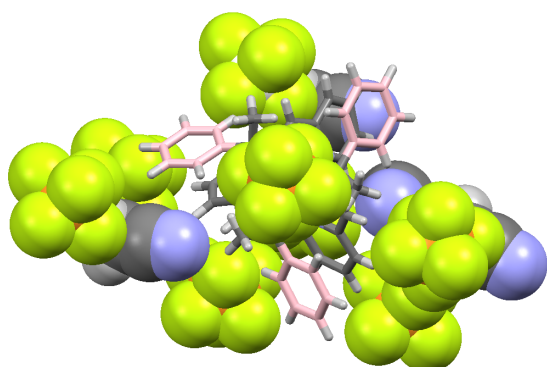
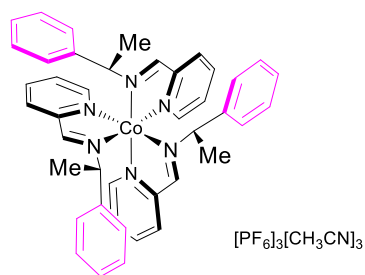
In contrast, this view perpendicular to the remaining pendant arene π -stack shows that it is relatively free of polar contacts. The same view of the cation in spacefill is shown below.



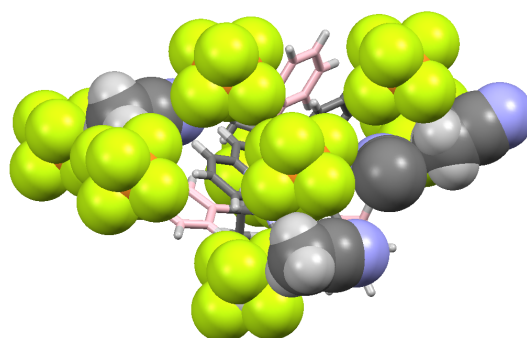
The following examples are re-analysis of all relevant previously published data.

Monometallic Co complex

CCDC code DAJHAZ, Figure 14 of *Dalton Trans.*, **2011**, *40*, 10416.



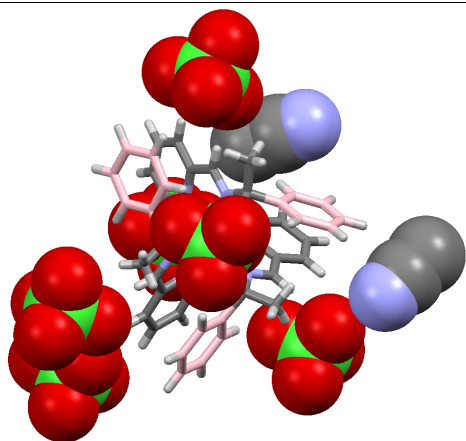
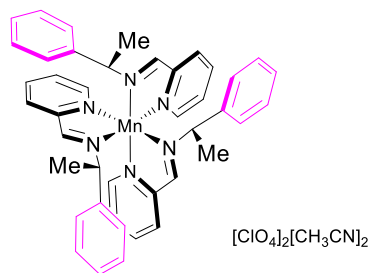
Viewed along the three-fold axis of the complex cation i.e. the same view as the ChemDraw structure above, the three pendant π -stacked arenes have only short contacts with C-H bonds of neighbouring complexes in the crystal (not shown here). In contrast, the edges of the π -stacks are surrounded by anions and acetonitrile solvent.



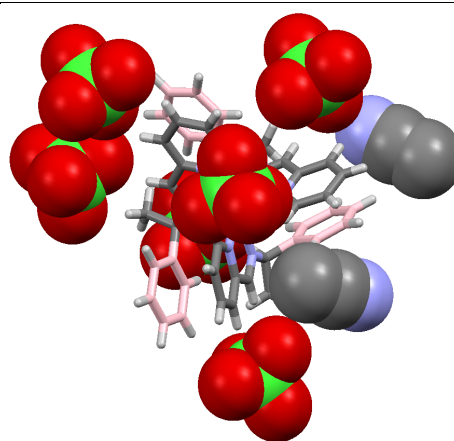
In this view from the "rear" of the complex, approximately along the same three-fold axis, the coordinated iminopyridine units are engulfed in anions and solvent.

Monometallic Mn complex

CCDC code DAJGEC, Figure 16 of *Dalton Trans.*, **2011**, *40*, 10416.

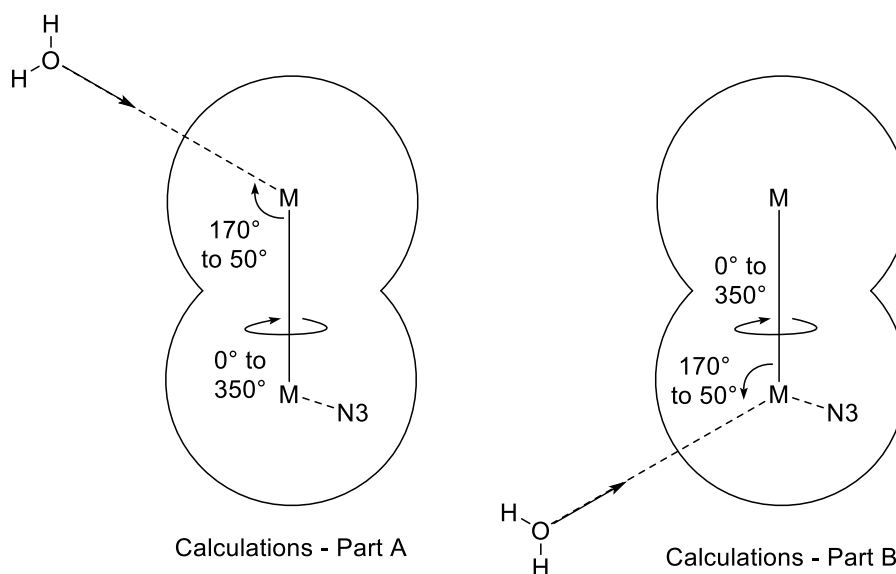


As for the Co structure above the edges of the π -stacks are surrounded by perchlorate anions and acetonitrile solvent, leaving the pendant arene faces free of such polar groups.



From the “rear” of the complex, while the coordinated iminopyridine units are surrounded by perchlorate and acetonitrile the packing is less dense than the Co structure above. This difference probably arises because the charge on the complex is 2+ rather than 3+ for the Co structure.

Hydrophobicity calculations



An array of polar coordinate calculations based on combinations of two frozen orientation angles and optimisation of the floating metal-oxygen distance.

Calculations were performed using the Firefly QC package,⁹ which is partially based on the GAMESS (US) source code.¹⁰ The computed structure¹ of the Zn(II) analogue of the cationic metallohelix unit in Δ -1 was used as the basis for this study since suitable Fe parameters were not available. The Zn(II) and Fe(II) compounds are isostructural.¹¹

A polar coordinates system (defining one metal as the origin, the primary axis as the two metal atoms, and one coordinating nitrogen N3 as the third point of reference) was used to define the position of the oxygen atom of a water molecule relative to the frozen atom positions of the tetra-cation Δ -1. In each calculation the position of the water oxygen was defined with a fixed azimuthal angle, (0° to 350° in 10° steps) relative to nitrogen atom 3, and a fixed polar angle (170° to 50° in 10° steps) and a freely floating radial distance from the origin (metal 1) starting at 10 \AA . The position of the two water hydrogen atoms were defined relative to the water oxygen atom (initially with standard bond lengths and angle) and allowed to move freely relative to the oxygen, including torsional angle relative to the origin (metal 1). An energy minimisation (AM1 semi-empirical basis set, with Fe changed to Zn due to lack of Fe parameters) was then performed keeping all atoms in complex cation Δ -1 fixed as well as the water

oxygen position defining azimuthal and radial angles, while origin (metal 1) oxygen distance and the positions of the water hydrogen atoms were allowed to vary. Thus 468 calculations were performed for all combinations of 36 azimuthal angles and 13 polar angles. Another 468 calculations were then performed defining the origin as the other metal (metal 2, with the primary axis as the two metal atoms, and one coordinating nitrogen N3 as the third point of reference) to complete the other half of the solvation “sphere” of the complex cation $\Delta\text{-1}$. The results from two of these calculations (polar angle 50 azimuthal, angle 190, and polar angle 50, azimuthal angle 310) were not included in the final results as they did not minimize to the reasonable energy gradient. Polar coordinates of the water oxygen atoms for each of the 934 (468x2 -2) calculations were then converted into xyz coordinates and plotted in MATLAB2016 using the scatter3 function, with the minimised energy as the colour scale. The difference between the highest and lowest energy in 25.5 kJmol⁻¹.

References

1. Faulkner, A. D.; Kaner, R. A.; Abdallah, Q. M. A.; Clarkson, G.; Fox, D. J.; Gurnani, P.; Howson, S. E.; Phillips, R. M.; Roper, D. I.; Simpson, D. H.; Scott, P.. *Nat. Chem.* **2014**, *6* (9), 797-803.
2. Howson, S. E.; Chmel, N. P.; Clarkson, G. J.; Deeth, R. J.; Simpson, D. H.; Scott, P., *Dalton Trans.* **2012**, *41* (15), 4477-4483.
3. Knight, C. A.; Hallett, J.; DeVries, A. L. *Cryobiology* **1988**, *25* (1), 55-60.
4. Schneider, C. A.; Rasband, W. S.; Eliceiri, K. W., *Nat Meth* **2012**, *9* (7), 671-675.
5. Coles, S. J.; Gale, P. A., *Chem. Sci.* **2012**, *3* (3), 683-689.
6. O. V. Dolomanov, L. J. B., R. J. Gildea, J. A. K. Howard, H. Puschmann., *J. App. Cryst.* **2009**, *42* (2), 339--341.
7. Sheldrick, G. M., *Acta Crystallogr., Sect. A* **2008**, *64* (1), 112-122.
8. Sheldrick, G. M., *Acta Cryst. C* **2015**, *71* (1), 3--8.
9. Granovsky, A. A. Firefly version 8. <http://classic.chem.msu.su/gran/firefly/index.html>.
10. Schmidt, M. W.; Baldrige, K. K.; Boatz, J. A.; Elbert, S. T.; Gordon, M. S.; Jensen, J. H.; Koseki, S.; Matsunaga, N.; Nguyen, K. A.; Su, S.; Windus, T. L.; Dupuis, M.; Montgomery, J. A.. *J. Comput. Chem.* **1993**, *14* (11), 1347-1363.
11. Howson, S. E.; Allan, L. E. N.; Chmel, N. P.; Clarkson, G. J.; Deeth, R. J.; Faulkner, A. D.; Simpson, D. H.; Scott, P.. *Dalton Trans.* **2011**, *40* (40), 10416-10433.